SECOND ORDER ARNOLDI REDUCTION: APPLICATION TO SOME ENGINEERING PROBLEMS

Jörg Lampe and Heinrich Voss

Hamburg University of Technology, Institute of Numerical Simulation,
D-21071 Hamburg, Federal Republic of Germany,
{joerg.lampe,voss}@tu-harburg.de

Abstract

A standard approach to model reduction of second order linear dynamical systems is to rewrite the system as an equivalent first order system and then employ Krylov subspace techniques for model reduction. Recently the Second Order Arnoldi Reduction (SOAR) method was presented by Bai and Su which constructs the projection to a second order Krylov subspace thus preserving the structure of the underlying problem. In this paper we demonstrate the superior numerical behavior of the SOAR-algorithm upon the first order methods for four engineering problems from different areas.

Keywords: order reduction, second order Krylov subspace, second order Arnoldi method

AMS Subject Classification: 65F15, 65F30, 65F50, 65F99

1 Introduction

Second order systems appear in various fields of engineering applications. Common examples are structural analysis, acoustics, electromagnetics or

microelectromechanical systems (MEMS). In the time domain a continuous time-invariant single-input single-output second order system (SISO system) is described by

$$\begin{aligned} \boldsymbol{M}\ddot{\boldsymbol{q}}(t) + \boldsymbol{D}\dot{\boldsymbol{q}}(t) + \boldsymbol{K}\boldsymbol{q}(t) &= \boldsymbol{b}u(t), \\ y(t) &= \boldsymbol{\ell}^H \boldsymbol{q}(t) \end{aligned} \tag{1.1}$$

with the initial conditions $\boldsymbol{q}(\boldsymbol{0}) = \boldsymbol{q}_0$ and $\dot{\boldsymbol{q}}(\boldsymbol{0}) = \dot{\boldsymbol{q}}_0$. Here $\boldsymbol{q}(t) \in \mathbb{C}^N$ is the vector of state variables with N being the state-space dimension.

The dimension N of those systems can be very large, and therefore it is necessary to obtain reduced order models of much smaller dimension which retain important properties of the original systems. A common approach for reducing the dimension of a higher order system is to linearize it, i.e. to replace it by an equivalent first order system, and to apply techniques based on moment matching or balanced truncation. Surveys of these methods can be found in [1, 2, 8]. However, this approach has two major disadvantages, the dimension is further increased and the structure of the original system is not preserved within the reduced model and it has no physical meaning.

Recently, a Second Order Arnoldi Reduction algorithm (SOAR-algorithm) was proposed by Bai and Su, which is an elegant and efficient way of reducing second order systems and keeping their second order structure. In this paper we will shortly describe this approach, and we will demonstrate its superior numerical behavior for four examples from different areas of engineering applications.

2 Order reduction via projection

Assuming homogeneous initial conditions $\boldsymbol{q}(\boldsymbol{0}) = \dot{\boldsymbol{q}}(\boldsymbol{0}) = \boldsymbol{0}$ and $u(0) = 0$, the second order system (1.1) in time domain can be represented equivalently as

$$\begin{aligned} s^2\boldsymbol{M}\tilde{\boldsymbol{q}}(s) + s\boldsymbol{D}\tilde{\boldsymbol{q}}(s) + \boldsymbol{K}\tilde{\boldsymbol{q}}(s) &= \boldsymbol{b}\tilde{u}(s), \\ \tilde{y}(s) &= \boldsymbol{\ell}^H \tilde{\boldsymbol{q}}(s) \end{aligned} \tag{2.1}$$

in frequency domain. Here $\tilde{\boldsymbol{q}}(s)$, $\tilde{u}(s)$ and $\tilde{y}(s)$ are the Laplace transforms of $\boldsymbol{q}(t)$, $u(t)$ and $y(t)$, respectively.

By eliminating $\tilde{\boldsymbol{q}}(s)$, one obtains the input-output behavior $\tilde{y}(s) = h(s)\tilde{u}(s)$ of the system, with

$$h(s) = \boldsymbol{\ell}^H(s^2\boldsymbol{M} + s\boldsymbol{D} + \boldsymbol{K})^{-1}\boldsymbol{b} \tag{2.2}$$

as the transfer function of (1.1). Physically meaningful values are $s = j\omega$ with $\omega \geq 0$.

We assume that $\boldsymbol{K}$ is nonsingular (otherwise we consider the shifted problem, replacing s by $s + s_0$ for some suitable s_0). Then h has the power series expansion

$$h(s) = m_0 + m_1 s + m_2 s^2 + \ldots = \sum_{k=0}^{\infty} m_k s^k, \tag{2.3}$$

where the m_k are called moments of h at the expansion point $s_0 = 0$.

A simple, but powerful approach for constructing reduced order models is moment matching, i.e. to determine a reduced model of much smaller dimension $n \ll N$ such that the corresponding transfer function

$$h_n(s) = m_0^{(n)} + m_1^{(n)} s + m_2^{(n)} s^2 + \ldots = \sum_{k=0}^{\infty} m_k^{(n)} s^k \tag{2.4}$$

satisfies $m_j = m_j^{(n)}$, $j = 0, 1, \ldots$ for as many leading moments as possible. Although the approximation is determined via a local property it usually has excellent approximation properties in large domains which may even contain poles.

We recall the construction of a reduced order model by linearization. Consider the first order system

$$\begin{aligned} \boldsymbol{C}\dot{\boldsymbol{x}}(t) + \boldsymbol{G}\boldsymbol{x}(t) &= \hat{\boldsymbol{b}}u(t), \\ y(t) &= \hat{\boldsymbol{\ell}}^H\boldsymbol{x}(t) \end{aligned} \tag{2.5}$$

with

$$\boldsymbol{C} = \begin{bmatrix} \boldsymbol{D} & \boldsymbol{M} \\ -\boldsymbol{I} & \boldsymbol{0} \end{bmatrix}, \boldsymbol{G} = \begin{bmatrix} \boldsymbol{K} & \boldsymbol{0} \\ \boldsymbol{0} & \boldsymbol{I} \end{bmatrix}, \hat{\boldsymbol{b}} = \begin{bmatrix} \boldsymbol{b} \\ \boldsymbol{0} \end{bmatrix}, \hat{\boldsymbol{\ell}} = \begin{bmatrix} \boldsymbol{\ell} \\ \boldsymbol{0} \end{bmatrix}, \boldsymbol{x}(t) = \begin{bmatrix} \boldsymbol{q}(t) \\ \dot{\boldsymbol{q}}(t) \end{bmatrix}$$

which is equivalent to (1.1). Then it is easily seen (cf. [4]) that (1.1) and (2.5) have identical transfer functions. Hence,

$$h(s) = \hat{\boldsymbol{\ell}}^H (s\boldsymbol{C} + \boldsymbol{G})^{-1}\hat{\boldsymbol{b}} = \hat{\boldsymbol{\ell}}^H (\boldsymbol{I} + s\boldsymbol{G}^{-1}\boldsymbol{C})^{-1}(\boldsymbol{G}^{-1}\hat{\boldsymbol{b}}), \tag{2.6}$$

and the Neumann series expansion of $(\boldsymbol{I} + s\boldsymbol{G}^{-1}\boldsymbol{C})^{-1}$ immediately yields

$$m_k = \hat{\boldsymbol{\ell}}^H (-\boldsymbol{G}^{-1}\boldsymbol{C})^k (\boldsymbol{G}^{-1}\hat{\boldsymbol{b}}), \quad k = 0, 1, 2, \ldots, n-1. \tag{2.7}$$

This representation suggests to construct a reduced order model which matches the leading moments by projecting (2.5) to the Krylov subspace

$$\mathcal{K}_n(-\boldsymbol{G}^{-1}\boldsymbol{C}, \hat{\boldsymbol{r}}_0) = \operatorname{span}\{\hat{\boldsymbol{r}}_0, -\boldsymbol{G}^{-1}\boldsymbol{C}\hat{\boldsymbol{r}}_0, \ldots, (-\boldsymbol{G}^{-1}\boldsymbol{C})^{n-1}\hat{\boldsymbol{r}}_0\}$$

with $\hat{\boldsymbol{r}}_0 = \boldsymbol{G}^{-1}\hat{\boldsymbol{b}}$.

An approach for computing an orthonormal basis of $\mathcal{K}_n(-\boldsymbol{G}^{-1}\boldsymbol{C}, \hat{\boldsymbol{r}}_0)$ and the projection of $-\boldsymbol{G}^{-1}\boldsymbol{C}$ to the Krylov space is the Arnoldi-method:

Algorithmus 2.1 Arnoldi-algorithm

1: $\boldsymbol{v}_1 = \hat{\boldsymbol{r}}_0/\|\hat{\boldsymbol{r}}_0\|_2$, $\boldsymbol{V}_1 = [\boldsymbol{v}_1]$;
2: **for** $j = 1, 2, \ldots, n$ **do**
3: $\quad \boldsymbol{r} = -\boldsymbol{G}^{-1}\boldsymbol{C}\boldsymbol{v}_j$
4: $\quad \boldsymbol{h}_j = \boldsymbol{V}_j^H \boldsymbol{r}$
5: $\quad \boldsymbol{r} = \boldsymbol{r} - \boldsymbol{V}_j \boldsymbol{h}_j$
6: $\quad h_{j+1,j} = \|\boldsymbol{r}\|_2$
7: $\quad \boldsymbol{v}_{j+1} = \boldsymbol{r}/h_{j+1,j}$, $\boldsymbol{V}_{j+1} = [\boldsymbol{V}_j \quad \boldsymbol{v}_{j+1}]$
8: **end for**

Then the upper Hessenberg matrix $\boldsymbol{H}_n = (h_{ij})$ generated in the Arnoldi-method is the orthogonal projection

$$\boldsymbol{H}_n = \boldsymbol{V}_n^H (-\boldsymbol{G}^{-1}\boldsymbol{C})\boldsymbol{V}_n$$

of $-\boldsymbol{G}^{-1}\boldsymbol{C}$ to the Krylov space $\mathcal{K}_n(-\boldsymbol{G}^{-1}\boldsymbol{C}, \hat{\boldsymbol{r}}_0)$, and the first n moments of h and

$$h_n(s) := \hat{\boldsymbol{\ell}}_n^H (\boldsymbol{I} - s\boldsymbol{H}_n)^{-1}\hat{\boldsymbol{b}}_n, \ \hat{\boldsymbol{\ell}}_n = \boldsymbol{V}_n^H \hat{\boldsymbol{\ell}}, \ \hat{\boldsymbol{b}}_n = \boldsymbol{V}_n^H \boldsymbol{G}^{-1}\hat{\boldsymbol{b}}$$

are identical, [10].

A drawback of this approach is that the corresponding linear system

$$\begin{aligned} -\boldsymbol{H}_n\dot{\boldsymbol{z}}(t) + \boldsymbol{z}(t) &= \hat{\boldsymbol{b}}_n u(t), \\ y_n(t) &= \hat{\boldsymbol{\ell}}_n^H \boldsymbol{z}(t) \end{aligned} \tag{2.8}$$

does not preserve the structure of a second order system.

This disadvantage can be overcome by projecting the second order system (1.1) directly to a second order Krylov subspace which was first introduced by Su and Craig [11] and later by Bai and Su [3, 4, 5] in the more explicit form given below.

We take advantage of the special structure of the matrix

$$-\boldsymbol{G}^{-1}\boldsymbol{C} = \begin{bmatrix} -\boldsymbol{K}^{-1}\boldsymbol{D} & -\boldsymbol{K}^{-1}\boldsymbol{M} \\ \boldsymbol{I} & \boldsymbol{0} \end{bmatrix} =: \begin{bmatrix} \boldsymbol{A} & \boldsymbol{B} \\ \boldsymbol{I} & \boldsymbol{0} \end{bmatrix}.$$

Then the moments

$$m_k = \hat{\boldsymbol{\ell}}^H(-\boldsymbol{G}^{-1}\boldsymbol{C})^k(\boldsymbol{G}^{-1}\hat{\boldsymbol{b}}) = (\boldsymbol{\ell}, \boldsymbol{0}) \begin{bmatrix} \boldsymbol{A} & \boldsymbol{B} \\ \boldsymbol{I} & \boldsymbol{0} \end{bmatrix}^k \begin{bmatrix} \boldsymbol{K}^{-1}\boldsymbol{b} \\ \boldsymbol{0} \end{bmatrix}$$

are given by

$$m_k = \boldsymbol{\ell}^H \boldsymbol{r}_k \tag{2.9}$$

with

$$\begin{aligned} \boldsymbol{r}_0 &= \boldsymbol{K}^{-1}\boldsymbol{b} \\ \boldsymbol{r}_1 &= \boldsymbol{A}\boldsymbol{r}_0 \\ \boldsymbol{r}_k &= \boldsymbol{A}\boldsymbol{r}_{k-1} + \boldsymbol{B}\boldsymbol{r}_{k-2} \quad \text{for} \quad k \geq 2. \end{aligned}$$

$\{\boldsymbol{r}_k\}$ is called a second order Krylov vector sequence, and the subspace spanned by this sequence is called second order Krylov subspace

$$\mathcal{G}_n(\boldsymbol{A}, \boldsymbol{B}, \boldsymbol{r}_0) := \text{span}\{\boldsymbol{r}_0, \boldsymbol{r}_1, \ldots, \boldsymbol{r}_{n-1}\}. \tag{2.10}$$

For an orthonormal basis $\boldsymbol{Q}_n$ of $\mathcal{G}_n(\boldsymbol{A}, \boldsymbol{B}, \boldsymbol{r}_0)$ we consider the projected linear system

$$\begin{aligned} \boldsymbol{M}_n \ddot{\boldsymbol{z}}_n(t) + \boldsymbol{D}_n \dot{\boldsymbol{z}}_n(t) + \boldsymbol{K}_n \boldsymbol{z}(t) &= \boldsymbol{b}_n u(t), \\ \tilde{y}(t) &= \boldsymbol{\ell}_n^H z(t) \end{aligned} \tag{2.11}$$

with $\boldsymbol{M}_n = \boldsymbol{Q}_n^H \boldsymbol{M} \boldsymbol{Q}_n$, $\boldsymbol{D}_n = \boldsymbol{Q}_n^H \boldsymbol{D} \boldsymbol{Q}_n$, $\boldsymbol{K}_n = \boldsymbol{Q}_n^H \boldsymbol{K} \boldsymbol{Q}_n$, $\boldsymbol{b}_n = \boldsymbol{Q}_n^H \boldsymbol{b}$ and $\boldsymbol{\ell}_n = \boldsymbol{Q}_n^H \boldsymbol{\ell}$, which not only preserves the structure of a second order linear system, but it also keeps symmetry and definiteness properties of the matrices $\boldsymbol{M}$, $\boldsymbol{D}$, and $\boldsymbol{K}$.

The following moment matching Theorem was proved in [4].

Theorem 2.1 *Let*

$$\tilde{h}_n(s) = \boldsymbol{\ell}_n^H (s^2 \boldsymbol{M}_n + s \boldsymbol{D}_n + \boldsymbol{K}_n)^{-1} \boldsymbol{b}_n = \sum_{k=0}^{\infty} \tilde{m}_k^{(n)} s^k. \tag{2.12}$$

Then the leading n moments of $h(s)$ and $\tilde{h}_n(s)$ are equal, i.e. $m_k = \tilde{m}_k^{(n)}$ for $k = 0, 1, \ldots, n-1$.

If $\boldsymbol{M}$, $\boldsymbol{D}$, and $\boldsymbol{K}$ are Hermitian, and $\boldsymbol{b} = \boldsymbol{\ell}$, then the first $2n$ moments of $h(s)$ and $\tilde{h}_n(s)$ coincide, i.e. $\tilde{h}_n$ is a Padé approximation of $h(s)$.

An orthonormal basis of the second order Krylov space $\mathcal{G}_n$ can be determined by *Second Order Arnoldi Reduction*-method (*SOAR*-method for short) which was introduced by Bai and Su in [5].

The SOAR-algorithm 2.2 with starting vector $\boldsymbol{r}_0$ breaks down if and only if the Arnoldi-algorithm 2.1 with starting vector $\hat{\boldsymbol{r}}_0$ breaks down as shown in [5] by Bai and Su. In the same paper a memory saving version of the algorithm 2.2 is presented which avoids saving the auxiliary vectors $\boldsymbol{p}_j$. An extension of the SOAR-algorithm concerning the dimension reduction of multi-input multi-output second order systems (taking into account deflations in a block second order Krylov subspace) is contained in [9]. Some work has been done to extend the SOAR-algorithm to higher order dynamical systems and the polynomial eigenvalue problem, respectively, [7, 9].

Algorithmus 2.2 SOAR-algorithm

$\boldsymbol{q}_1 = \boldsymbol{u}/\|\boldsymbol{u}\|_2$
$\boldsymbol{p}_1 = \boldsymbol{0}$
for $j = 1, 2, \ldots, n-1$ **do**
    $\boldsymbol{r} = \boldsymbol{A}\boldsymbol{q}_j + \boldsymbol{B}\boldsymbol{p}_j$
    $\boldsymbol{s} = \boldsymbol{q}_j$
    for $i = 1, 2, \ldots, j$ **do**
        $t_{ij} = \boldsymbol{q}_i^H \boldsymbol{r}$
        $\boldsymbol{r} = \boldsymbol{r} - \boldsymbol{q}_i t_{ij}$
        $\boldsymbol{s} = \boldsymbol{s} - \boldsymbol{p}_i t_{ij}$
    end for
    $t_{j+1,j} = \|\boldsymbol{r}\|_2$
    if $t_{j+1,j} = 0$ **then**
        if $\boldsymbol{s} \in span\{\boldsymbol{p}_i \mid i : \boldsymbol{q}_i = \boldsymbol{0}, 1 \leq i \leq j\}$ **then**
            breakdown
        else deflation:
            reset $t_{j+1,j} = 1$
            $\boldsymbol{q}_{j+1} = \boldsymbol{0}$
            $\boldsymbol{p}_{j+1} = \boldsymbol{s}$
        end if
    else
        $\boldsymbol{q}_{j+1} = \boldsymbol{r}/t_{j+1,j}$
        $\boldsymbol{p}_{j+1} = \boldsymbol{s}/t_{j+1,j}$
    end if
end for

3 Numerical examples

In this section, four numerical examples are presented to demonstrate the superior properties of the SOAR-algorithm. The approximation quality of the SOAR-algorithm 2.2 is compared to the Arnoldi-procedure 2.1 applied to the linearized model. All experiments were run in MATLAB 7.0.4 on a Linux-cluster of the institute.

3.1 Accelerator cavity

This example is a quadratic eigenvalue problem (QEP). It is derived from discretized Maxwell-equations of electromagnetic cavities in accelerators. In the case of an open cavity the vector wave equation with waveguide boundary conditions can be modeled by a nonlinear eigenvalue problem:

$$\boldsymbol{K}\boldsymbol{x} + i\sum_{j=1}^{d}\sqrt{k^2 - k_{cj}^2}\boldsymbol{W}_j\boldsymbol{x} = k^2\boldsymbol{M}\boldsymbol{x}, \tag{3.1}$$

where d is the number of waveguides which are leading into this cavity, and k_{cj} are coefficients of the corresponding waveguides. The eigenvalues are the resonant frequencies and the eigenvectors describe the corresponding electromagnetic field. Eigenvalues with smallest magnitude are of interest.

We assume $k_{cj} = 0$, $j = 1, \ldots, d$ which simplifies (3.1) to the quadratic eigenvalue problem

$$\left(\lambda^2\boldsymbol{M} - i\lambda\sum_{j=1}^{d}\boldsymbol{W}_j - \boldsymbol{K}\right)\boldsymbol{x} = \boldsymbol{0}, \tag{3.2}$$

with $\lambda = \sqrt{k^2}$.

In particular we consider a finite element model with $N = 9956$ degrees of freedom of a cavity connecting two waveguides, which is named „gun-cavity“ and is shown in Figure 1. Hence the quadratic eigenproblem (3.2) obtains the form

$$\left(\lambda^2\boldsymbol{M} - i\lambda(\boldsymbol{W}_1 + \boldsymbol{W}_2) - \boldsymbol{K}\right)\boldsymbol{x} = \boldsymbol{0}. \tag{3.3}$$

Figure 1 FEM-model of gun-cavity $N = 9956$

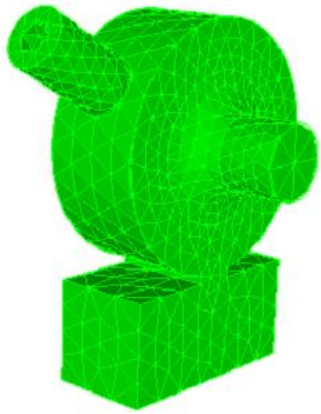

The system matrices have got the following properties:

$N = 9956$	$\|\cdot\|_1$	real	sym.	pos. def.	nnz
$\boldsymbol{M}$	17.04	yes	yes	yes	148318
$\boldsymbol{W}_1 + \boldsymbol{W}_2$	0.95	yes	yes	no	350
$\boldsymbol{K}$	14.75	yes	yes	no	148308

Since all matrices are real, the spectrum of (3.3) is symmetric about the imaginary axis. Diagram 2(a) shows 600 eigenvalues with smallest magnitude which have been calculated via a projection method of high order and which serve as reference values when evaluating the approximations.

Diagram 2(b) exhibits the approximate eigenvalues obtained by the SOAR-algorithm (triangles) and by the Arnoldi-procedure applied to the linearized problem (plus signs). In both cases the expansion point is chosen to be $s_0 = 0.07$, and the dimension of the reduced model is $n = 20$.

The eigenvalue approximations from the SOAR-algorithm preserve the symmetry about the imaginary axis which is not the case for for the Arnoldi-

Figure 2 Eigenvalues and SOAR/Arnoldi-approximations

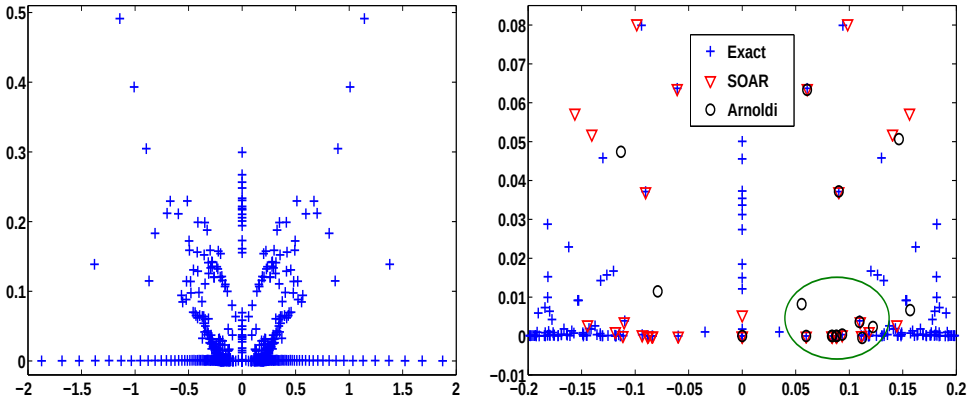

(a) 600 smallest eigenvalues

(b) SOAR/Arnoldi, $n = 20$, $s_0 = 0.07$

procedure (the Arnoldi-eigenvalues within the ellipse have no counterpart on the left side).

In the following we compare the accuracy of the approximations to eigenvalues with smallest magnitude obtained with the SOAR- and the Arnoldi-procedure. The two smallest eigenvalues with positive real part are

$$\begin{aligned}\lambda_1 &= 0.05979318129849 + 0.00000060564291 * i,\\ \lambda_2 &= 0.08377031861983 + 0.00001865296741 * i.\end{aligned}$$

The Arnoldi-procedure ($n = 10$) yields the approximations

$$\begin{aligned}\lambda_1^{Ar} &= \underline{0.05979322}105350 + \underline{0.00000070}031027 * i,\\ \lambda_2^{Ar} &= \underline{0.0835}6811958546 + \underline{0.0000}4068274681 * i\end{aligned}$$

and the SOAR-algorithm ($n = 10$)

$$\begin{aligned}\lambda_1^{S} &= \underline{0.05979318}141426 + \underline{0.00000060}548039 * i,\\ \lambda_2^{S} &= \underline{0.0837}9343875125 + \underline{0.0000}2471127141 * i\end{aligned}$$

where we have underlined the leading correct digits.

After $n = 20$ iterations 16 leading digits of λ_1^S and λ_1 match. The eigenvalue approximations with the SOAR-algorithm are more exact than the ones with the Arnoldi-procedure. The elapsed time for generating the orthonormal basis was $t_{Ar} = 25.1s$ with the Arnoldi-method and only $t_S = 7.7s$ with the SOAR-method.

3.2 Butterfly Gyroscope

The Butterfly Gyroscope is developed by the Imego Institute. It is a micro-electromechanical sensor for measuring inertia. More precisely, for measuring Coriolis acceleration. A special chip has been designed for this sensor. The schematic layout of the gyroscope and a picture of the finite element model is given in [6]. Basic equations from elastodynamics lead to a discretized model of the form:

$$\boldsymbol{M}\ddot{\boldsymbol{x}} + \boldsymbol{D}\dot{\boldsymbol{x}} + \boldsymbol{K}\boldsymbol{x} = \boldsymbol{b}\,u \tag{3.4}$$

$$\boldsymbol{y} = \boldsymbol{C}\boldsymbol{x}, \tag{3.5}$$

where $\boldsymbol{M}, \boldsymbol{D}, \boldsymbol{K} \in \mathbb{R}^{17361\times 17361}$, $\boldsymbol{C} \in \mathbb{R}^{12\times 17361}$ and $\boldsymbol{b} \in \mathbb{R}^{17361\times 1}$. This MIMO-system has got one input u and 12 outputs in $\boldsymbol{y}$. By taking into account only the last component of $\boldsymbol{y}$ the system reduces to a SISO-system:

$$h(s) = \boldsymbol{C}_{12}\big(s^2\boldsymbol{M} + s\boldsymbol{D} + \boldsymbol{K}\big)^{-1}\boldsymbol{b} \quad \text{mit} \quad \boldsymbol{C}_{12} = \boldsymbol{C}(12, 1:17361). \tag{3.6}$$

The damping matrix $\boldsymbol{D}$ is assumed to be $\boldsymbol{D} = \alpha\boldsymbol{K}$ with $\alpha = 10^{-6}$. Then the matrices $\boldsymbol{M}, \boldsymbol{D}$ and $\boldsymbol{K}$ have the following properties:

$N = 17361$	$\|\cdot\|_1$	real	pos. def.	nnz
$\boldsymbol{M}$	$3.8 * 10^{-7}$	yes	yes	340431
$\boldsymbol{D}$	$6.9 * 10^{3}$	yes	yes	1021159
$\boldsymbol{K}$	$6.9 * 10^{9}$	yes	yes	1021159

Approximating the transfer function by the SOAR- and Arnoldi-procedure we chose the expansion point $s_0 = 10^5$.

Figure 3 Bode plot SOAR/Arnoldi, $n = 20$, expansion point $s_0 = 10^5$

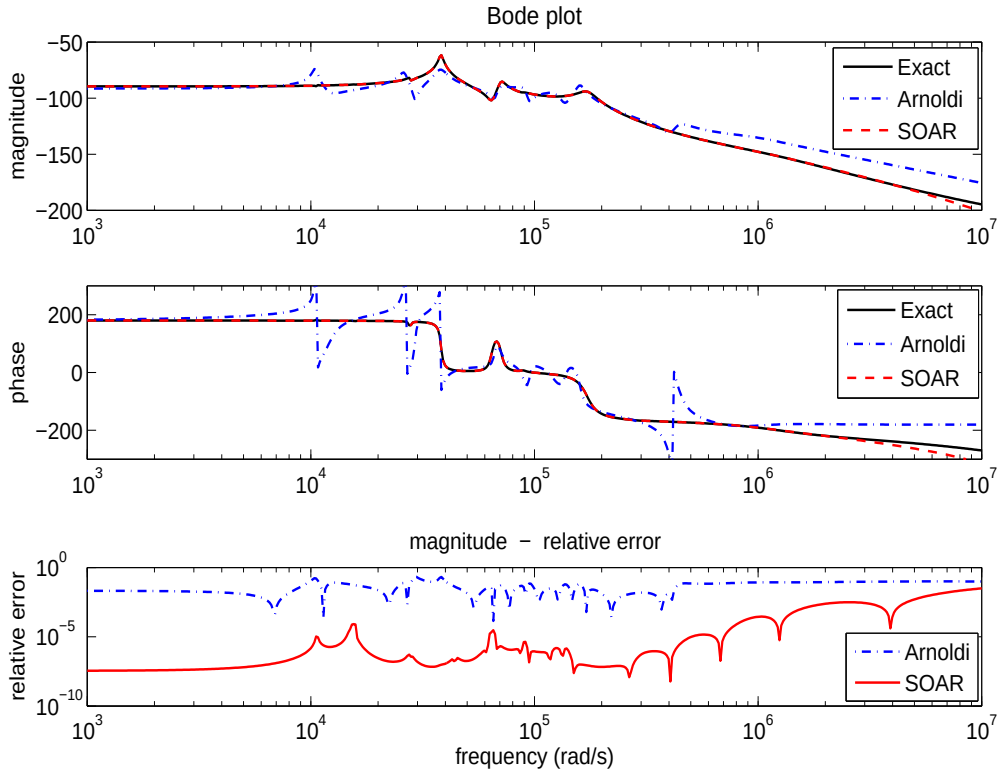

The upper two pictures of Figure 3 show the Bode plots of the transfer function $h(s)$ together with its approximations obtained with the SOAR- and the Arnoldi-method. The lower figure presents a plot of the relative errors as functions of the frequency. An approximation from a high order projection method ($n = 200$) has been taken as the reference transfer function.

The SOAR-based approximated transfer function is already very close to the exact solution over a wide range of frequency at a dimension of

$n = 20$. The relative error is superior by orders of magnitude compared to the Arnoldi-procedure. This behavior does not change with the dimension $n = 30$ of the reduced order model.

Figure 4 Bode plot SOAR/Arnoldi, $n = 30$, expansion point $s_0 = 10^5$

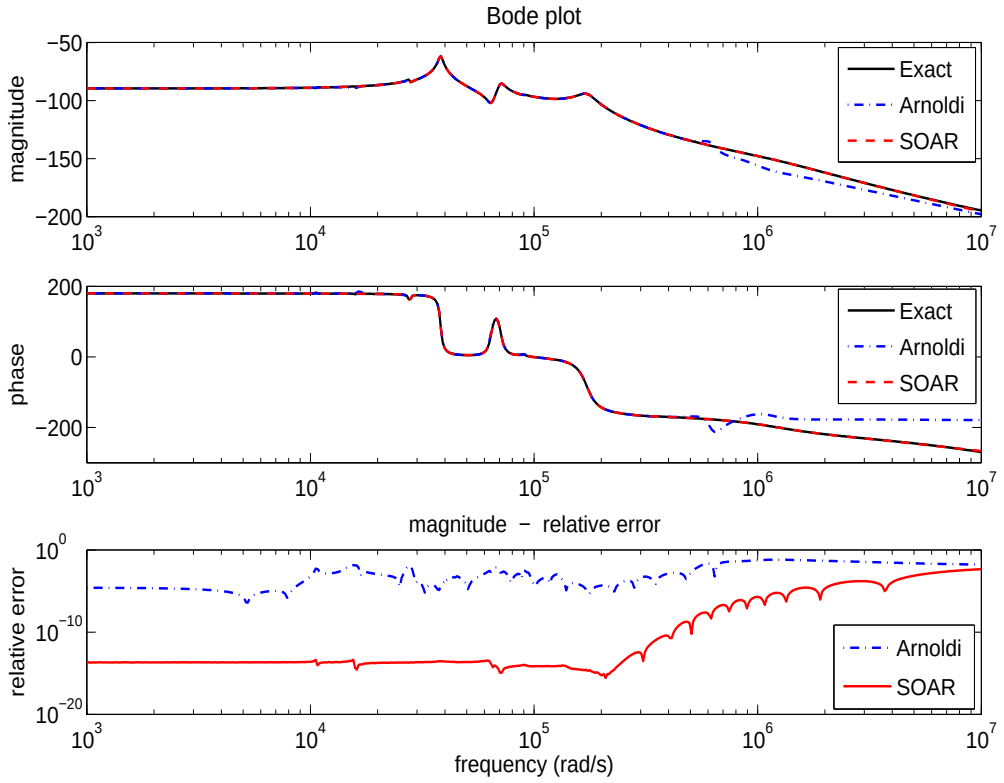

In Figure 4 the exact transfer function distinguishes from the one obtained by the SOAR-algorithm up to a frequency of $\omega = 2 * 10^5 rad/s$ only by a relative error of 10^{-14}. This approximation is clearly better than with the Arnoldi-procedure. The elapsed time of the SOAR-method is in both cases about half the time the Arnoldi-method needs to build up the or-

thonormal basis: The times of the algorithms for a reduced order of $n = 20$ are $t_{Ar} = 12.7s$ and $t_S = 5.1s$, and for an order of $n = 30$ the elapsed time for the Arnoldi-method is $t_{Ar} = 15.2s$ and for the SOAR-method $t_S = 6.4s$.

3.3 Vibrational analysis

This is an example from structural analysis. A part of a new breaking system from Bosch is examined. A rotating disk is decelerated by a brake unit and thus excites vibrations. Thereby it is possible to cause instabilities by certain breaking forces. The modeling is done via the conservation equations from mechanics. This results in a QEP of the form:

$$(\lambda^2 \boldsymbol{M} + \lambda \boldsymbol{D} + \boldsymbol{K})\boldsymbol{x} = \boldsymbol{0}. \tag{3.7}$$

The order of this problem is $N = 67986$. A FEM-model of the disk and the breaking unit is shown in figure 5. The task in this example is to determine

Figure 5 FEM-model of breaking system $N = 67986$

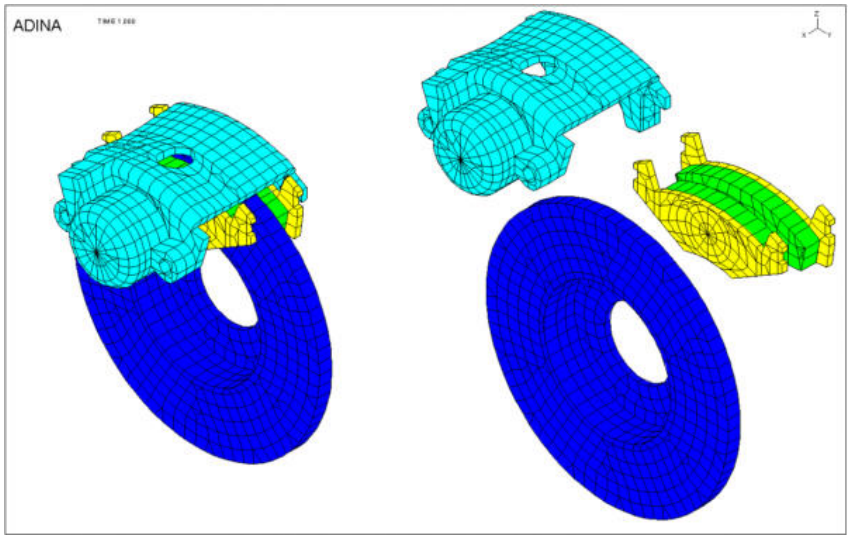

the „rightmost eigenvalues“, i.e. find out if there are eigenvalues within the

right half-plane. It should be noted that the SOAR-algorithm preserves the structure of the system matrices but not the stability in general.
The mass matrix $\boldsymbol{M}$ is fix, but the stiffness matrix $\boldsymbol{K}$ varies depending on the load. The damping matrix $\boldsymbol{D}$ is approximated with the help of Rayleigh-damping. The damping is assumed to be proportional to mass- and stiffness matrix, $\boldsymbol{D} = a\boldsymbol{M} + b\boldsymbol{K}$. The parameters a and b depend on eigenvalues of the undamped problem, $(\lambda^2\boldsymbol{M} + \boldsymbol{K}_0)\boldsymbol{x} = \boldsymbol{0}$. The following details specify the matrices:

$N = 67986$	$\|\cdot\|_1$	real	sym.	pos. def.	nnz
$\boldsymbol{M}$	0.06	yes	yes	yes	68150
$\boldsymbol{D}$	$2.2 * 10^9$	yes	no	no	4222874
$\boldsymbol{K}$	$5.6 * 10^{14}$	yes	no	no	4223355

Diagram 6(a) gives an overview of the eigenvalue distribution. It has been created with a higher order projection method ($n = 200$). Most of the eigenvalues are located in a circle around the point $s = -2.5 * 10^5$. Now, SOAR- and Arnoldi-procedure are used to calculate eigenvalue approximations close to the expansion point $s_0 = -10^4$. Having in mind the eigenvalue distribution in Figure 6(a) this should lead to approximated eigenvalues close to the origin. The result is shown in Figure 6(b) with a reduced order of $n = 40$. The SOAR-approximated eigenvalues are located on the circle from Figure 6(a), in contrast to the eigenvalue approximations with the Arnoldi-procedure. When the dimension n of the projection space increases these eigenvalues move towards this circle. An observation of the six smallest eigenvalues (in magnitude) yields:

Exact $[10^3]$	SOAR $[10^3]$	Arnoldi $[10^3]$
0.000000011	$-\underline{0.000000}022$	$\underline{0.0}1 - 1.22i$
-0.006427042	$-\underline{0.006427}009$	$\underline{0.0}1 + 1.22i$
$-0.005820228 - 1.1641222i$	$-\underline{0.005820}226 - \underline{1.164}1217i$	$-\underline{0.0}4 - \underline{1.}49i$
$-0.005820228 + 1.1641222i$	$-\underline{0.005820}226 + \underline{1.164}1217i$	$-\underline{0.0}4 + \underline{1.}49i$
$-0.007180567 - 1.4361041i$	$-\underline{0.007180}571 - \underline{1.436104}9i$	$-\underline{0.}26 - 2.64i$
$-0.007180567 + 1.4361041i$	$-\underline{0.007180}571 + \underline{1.436104}9i$	$-\underline{0.}26 + 2.64i$

The structure preserving SOAR-algorithm is clearly superior to the Arnoldi-method. The exact eigenvalues have been obtained again with a higher order projection method. It should be pointed out that the SOAR-algorithm indeed leads to better eigenvalue approximations but do not need to preserve the stability of the system (no eigenvalue with positive real-part is created with the SOAR-algorithm, although the model is instable). Most of the processing time was needed for computing the LU-decomposition of the matrix $\boldsymbol{K}$: $t_{LU} = 40s$. The times needed for the subsequent algorithms have been: $t_{Ar} = 50s$ for the Arnoldi-procedure and $t_S = 37s$ for the SOAR-procedure.

Figure 6 Eigenvalues and SOAR/Arnoldi-approximations

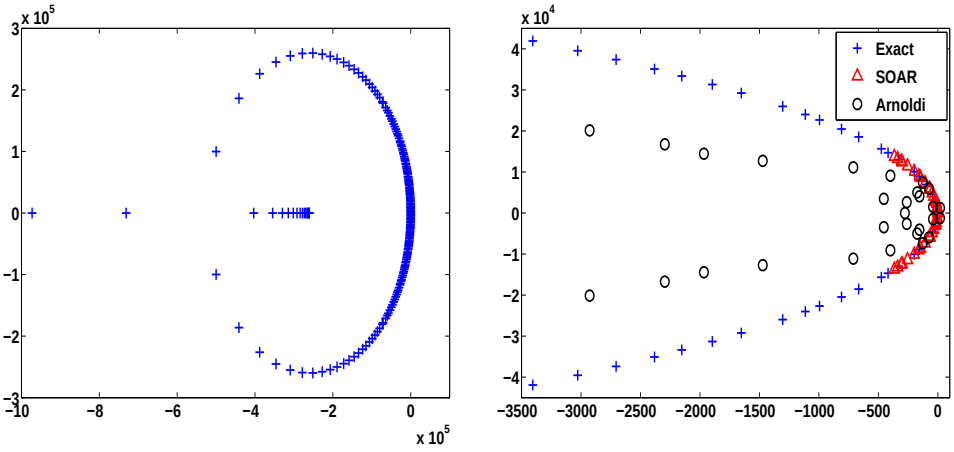

(a) Eigenvalue distribution, $s_0 = -10^5$ (b) SOAR/Arnoldi, $n = 40$, $s_0 = -10^4$

3.4 Sound radiation analysis

The last example has its origin in the model reduction of the exterior boundary value problem in acoustics. A vibrating three-dimensional body is going to be be analyzed. This body is a quarter-sphere. The time-harmonic pressure due to these vibrations can be determined with the Helmholtz-equation. The space that is examined in this example is infinite. The quarter-sphere

Figure 7 Discretized model of quarter-sphere $N = 17611$

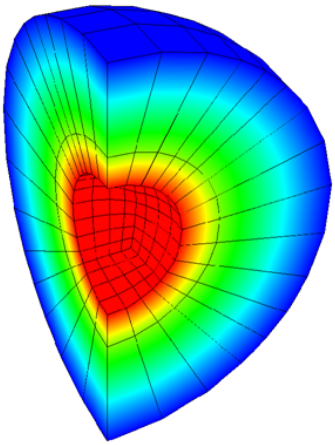

is divided into $N = 17611$ elements. The inner part is described via common finite elements whereas the outer part is described via half-infinite elements. The inner part of the quarter-sphere is excited by a homogeneous velocity. This example is called „the breathing sphere“. A discretization of the weak formulation of the exterior boundary value problem yields the following second order system:

$$\left(-\omega^2 \boldsymbol{M} + i\omega \boldsymbol{D} + \boldsymbol{K}\right) \boldsymbol{x} = \boldsymbol{b} u \tag{3.8}$$

$$y = \boldsymbol{\ell}^H \boldsymbol{x}. \tag{3.9}$$

The load vector $\boldsymbol{b}$ contains the normal-velocities of each element. The state vector $\boldsymbol{x}$ accords with the acoustic pressure on the corresponding elements. The output vector $\boldsymbol{\ell}$ picks a certain element out of $\boldsymbol{x}$, which is close to the inner part. The three system matrices exhibit following properties:

$N = 17611$	$\|\cdot\|_1$	real	sym.	pos. def.	nnz
$\boldsymbol{M}$	362	yes	yes	no	1071011
$\boldsymbol{D}$	291.4	yes	no	no	879697
$\boldsymbol{K}$	923.1	yes	no	no	1071011

SOAR- and Arnoldi-procedure are used for model reduction. The expansion point has been chosen to be $s_0 = 0.01$.

Figure 8 Bode plot SOAR/Arnoldi, $n = 10$, expansion point $s_0 = 0.1$

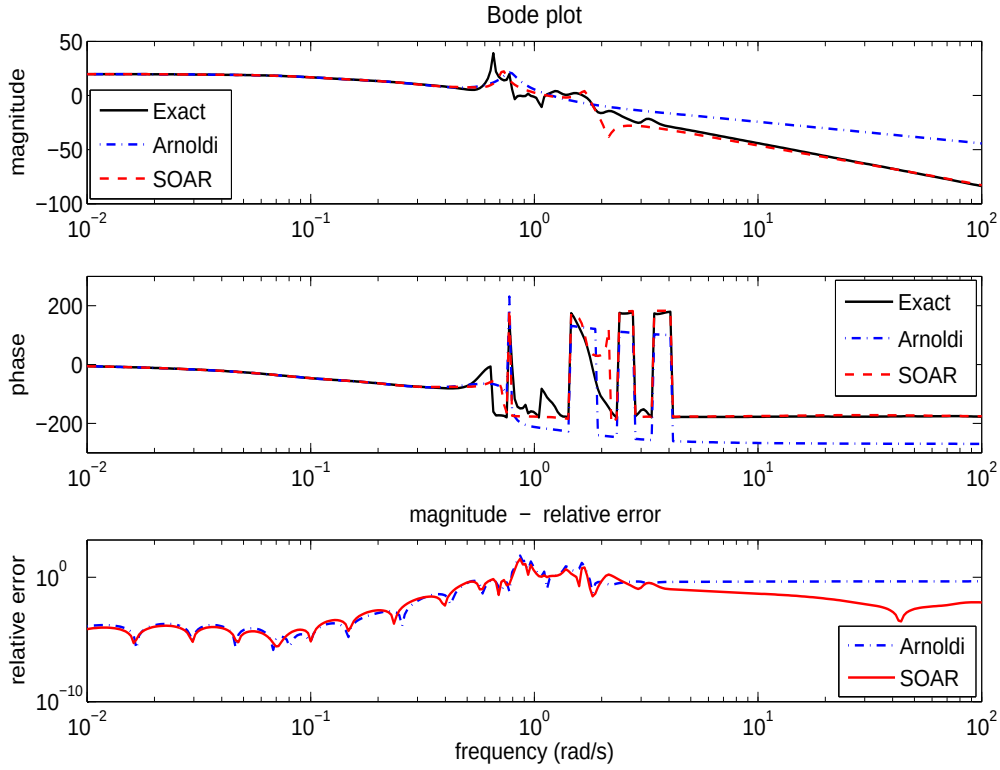

In Figure 8 the dimension of the reduced models is $n = 10$. Both order reduction methods yield good approximations up to a frequency of $\omega = 0.5 rad/s$. For higher frequencies SOAR- and Arnoldi-approximations are not exact. But for high frequencies the structure preserved transfer function (with the SOAR-procedure) is a much better approximation than the Arnoldi-approximation. Figure 9 shows the situation for a dimension of $n = 20$.

Figure 9 Bode plot SOAR/Arnoldi, $n = 20$, expansion point $s_0 = 0.1$

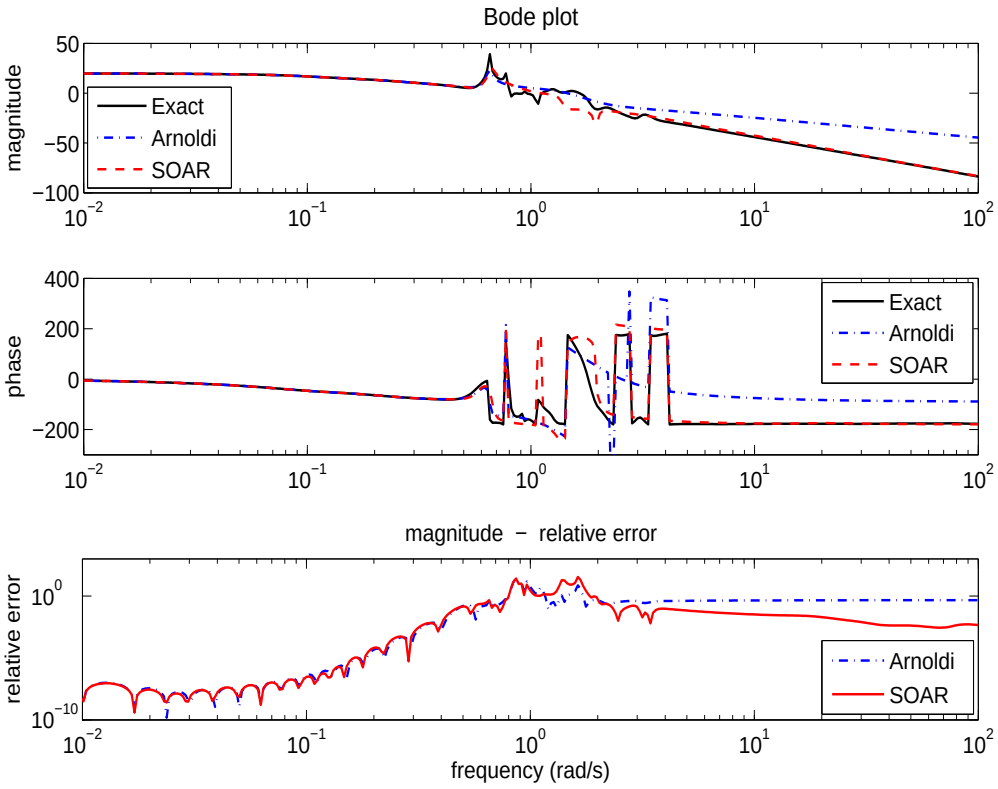

Up to a frequency of $\omega = 1rad/s$ the transfer function obtained via the Arnoldi-procedure is as good as the SOAR-based transfer function. For higher frequencies the structure preserved transfer function is closer to the exact one. Also the processing times are much better with the SOAR-algorithm. The elapsed times for creating the orthonormal bases of the reduced dimension $n = 10$ are $t_S = 12s$ for the SOAR-algorithm and $t_{Ar} = 37s$ for the Arnoldi-procedure. For the dimension of $n = 20$ the ratio is about the same: $t_S = 15s$ und $t_{Ar} = 43s$. Most of the time is needed again for the LU-decomposition. Because the Arnoldi-procedure has to factorize a matrix of double size, it needs significantly more time.

References

[1] A.C. Antoulas, D.C. Sorensen, and S. Gugercin. A survey of model reduction methods for large-scale systems. *Contemporary Mathematics*, 280:193–219, 2001.

[2] Z. Bai. Krylov subspace techniques for reduced-order modeling of large-scale dynamical systems. *Applied Numerical Mathematics*, 43:9–44, 2002.

[3] Z. Bai, K. Meerbergen, and Y. Su. Arnoldi methods for structure-preserving dimension reduction of second-order dynamical systems. In P. Benner, G. Golub, V. Mehrmann, and D. Sorensen, editors, *Dimension Reduction of Large-Scale Systems*, volume 45 of *Lecture Notes in Computational Science and Engineering*, pages 173 – 189, Berlin, 2005. Springer Verlag.

[4] Z. Bai and Y. Su. Dimension reduction of large-scale second-order dynamical systems via a second-order Arnoldi method. *SIAM J. Sci. Comp.*, 26:1692–1709, 2005.

[5] Z. Bai and Y. Su. Soar: A second-order Arnoldi method for the solution of the quadratic eigenvalue problem. *SIAM J. Matrix Anal. Appl.*, 26:640–659, 2005.

[6] D. Billger. The butterfly gyro. In P. Benner, G. Golub, V. Mehrmann, and D. Sorensen, editors, *Dimension Reduction of Large-Scale Systems*, volume 45 of *Lecture Notes in Computational Science and Engineering*, pages 349 – 352, Berlin, 2005. Springer Verlag.

[7] R. Freund. Krylov subspaces associated with higher-order linear dynamical systems. *BIT*, 45, 2005.

[8] R.W. Freund. Krylov-subspace methods for reduced-order modeling in circuit simulation. *J. Comput. Appl. Math.*, 123:395–421, 2000.

[9] J. Lampe. Modellreduktion für sehr große, dünn besetzte Systeme zweiter Ordnung mit dem Arnoldi-Verfahren. Master's thesis, Hamburg University of Technology, Institute of Numerical Simulation, 2005.

[10] R.-C. Li and Z. Bai. Structure-Preserving Model Reduction Using a Krylov Subspace Projection Formulation. *Communications in Mathematical Sciences*, 3:179 – 199, 2005.

[11] T.-J. Su and R.R. Craig Jr. Model Reduction and Control of Flexible Structures Using Krylov Vectors. *J. of Guidance, Control and Dynamics*, 14:260 – 267, 1991.